Evaluation of Predicted Knee-Joint Muscle Forces during Gait Using an Instrumented Knee Implant

Hyung J. Kim,[1] Justin W. Fernandez,[1] Massoud Akbarshahi,[1] Jonathan P. Walter,[2] Benjamin J. Fregly,[1,2] Marcus G. Pandy[1]

[1]Department of Mechanical Engineering, University of Melbourne, Carlton, Victoria 3010, Australia, [2]Department of Mechanical and Aerospace Engineering, University of Florida, Gainesville, Florida

Received 19 August 2008; accepted 5 February 2009
Published online 24 April 2009 in Wiley InterScience (www.interscience.wiley.com). DOI 10.1002/jor.20876

ABSTRACT: Musculoskeletal modeling and optimization theory are often used to determine muscle forces in vivo. However, convincing quantitative evaluation of these predictions has been limited to date. The present study evaluated model predictions of knee muscle forces during walking using in vivo measurements of joint contact loading acquired from an instrumented implant. Joint motion, ground reaction force, and tibial contact force data were recorded simultaneously from a single subject walking at slow, normal, and fast speeds. The body was modeled as an 8-segment, 21-degree-of-freedom articulated linkage, actuated by 58 muscles. Joint moments obtained from inverse dynamics were decomposed into leg-muscle forces by solving an optimization problem that minimized the sum of the squares of the muscle activations. The predicted knee muscle forces were input into a 3D knee implant contact model to calculate tibial contact forces. Calculated and measured tibial contact forces were in good agreement for all three walking speeds. The average RMS errors for the medial, lateral, and total contact forces over the entire gait cycle and across all trials were 140 ± 40 N, 115 ± 32 N, and 183 ± 45 N, respectively. Muscle coordination predicted by the model was also consistent with EMG measurements reported for normal walking. The combined experimental and modeling approach used in this study provides a quantitative framework for evaluating model predictions of muscle forces in human movement. © 2009 Orthopaedic Research Society. Published by Wiley Periodicals, Inc. J Orthop Res 27:1326–1331, 2009

Keywords: x-ray fluoroscopy; total knee replacement; musculoskeletal model; tibiofemoral; biomechanics

Walking is important for human health, and independent ambulation predicts quality of life. The study and treatment of walking disorders would be more effective if the forces developed by muscles in individual patients could be determined reliably. Accurate knowledge of muscle forces would allow clinicians to diagnose and treat a range of musculoskeletal disorders that are commonly seen in patients suffering from stroke, cerebral palsy, and osteoarthritis. Accurate information on the loading patterns incurred by the muscles and bones would also inform the design of joint replacements and tissue-engineered constructs that are developed to replace soft tissues, such as ligaments and cartilage, which are frequently damaged as a result of injury.

Because noninvasive measurement of muscle forces in living subjects is currently not possible, computational modeling is often used to determine these quantities indirectly. One of the major challenges of the modeling approach is the nonunique character of the muscle force solutions. Because each joint is spanned by several muscles, a net joint torque can be produced by an infinite combination of muscle forces. Many studies combined musculoskeletal modeling and optimization techniques to determine muscle forces in various tasks, including walking.[1] In most of these studies, the model calculations were validated by comparing the time histories of the muscle forces predicted by the model against in vivo measurements of muscle activity obtained from electromyography (EMG). Internal contact force measurements obtained from instrumented joint replacements offer a more quantitative means of evaluating model calculations of muscle forces. Since muscle forces contribute significantly to articular contact loading at joints,[2] accurate model predictions of joint contact loading would imply that estimates of the corresponding muscle forces are also reasonable.

A number of studies used direct measurements of joint contact forces obtained from instrumented implants to evaluate model predictions of muscle and joint loading during human movement.[3–8] Muscle forces calculated by a musculoskeletal model predicted hip contact forces during walking in close agreement with measurements made by a force-measuring hip implant.[5] When the same model was applied to the knee, however, predicted contact forces during gait were much higher than previously reported knee contact forces.[7] Some researchers also attempted to validate model predictions of knee-joint loading against measurements obtained from instrumented joint replacements implanted into cadaver specimens.[9] The main difficulty with this approach is that the complex loading patterns experienced by the knee in tasks such as walking cannot easily be reproduced in a cadaver model. To our knowledge, no study has evaluated model calculations of articular contact forces at the knee against direct measurements of knee-joint loading obtained in vivo from the same subject.

The purpose of the present study was to evaluate model predictions of knee muscle forces during walking using in vivo measurements of joint contact loading acquired from a patient fitted with an instrumented knee implant. Quantitative comparisons of computed knee-joint loading against measurements of the medial, lateral, and total tibial contact forces were used to evaluate the accuracy with which a subject-specific musculoskeletal model of the lower limb could determine the forces developed by the knee muscles during gait.

METHODS

Previously reported data recorded from a single male patient (age, 80 years; mass, 68 kg; height, 1.7 m) 8 months

Correspondence to: M.G. Pandy (T: +61 3 8344 4054; F: +61 3 8344 4290); E-mail: pandym@unimelb.edu.au

subsequent to total knee arthroplasty (TKA) were used.[10,11] Joint motion, ground forces, and tibial contact forces were measured simultaneously for level walking at three speeds: slow (0.80 ± 0.05 m/s), normal (1.24 ± 0.03 m/s), and fast (1.52 ± 0.04 m/s). Data were recorded for three trials at each speed. Single-plane fluoroscopy was also used to measure the relative positions of the implant components as the subject walked on a treadmill (hands resting on handlebars) at his normal speed.[12] Data from the over-ground and treadmill trials were synchronized using the total tibial forces measured in both sets of experiments. Details of the gait experiments can be found in Zhao et al.[10,11]

Leg-muscle forces were calculated using a model of the body very similar to that reported by Anderson and Pandy.[13] The body was modeled as an 8-segment, 21-degree-of-freedom articulated linkage, actuated by 58 muscles (Fig. 1, whole-body model). Segment inertial properties were scaled to the dimensions of the TKA patient using anthropometric measures derived from five adult male subjects.[14] The locations of the joint centers and the orientations of the joint axes were found by minimizing the differences between the positions of surface markers located on the subject and virtual markers defined in the model.[15] The force-generating properties, attachment sites, and paths of all the muscles in the model were the same as those identified by Anderson and Pandy,[16] except that hamstrings and gastrocnemius were each divided into a medial and lateral portion.

Because the knee was represented as a hinge in the whole-body model, the moments induced at the knee by those muscles with lines of action acting out of the sagittal plane could not be included in the calculation of the net joint torques. An external moment was therefore applied about the AP axis of the knee to simulate the effect of the knee adduction moment during gait. This moment was found by computing the cross-product of the resultant ground reaction force vector and a vector directed from the knee-joint center to one point on the line of action of the ground force. The component of this moment vector acting about the AP axis was used as an estimate of the external knee adduction moment.

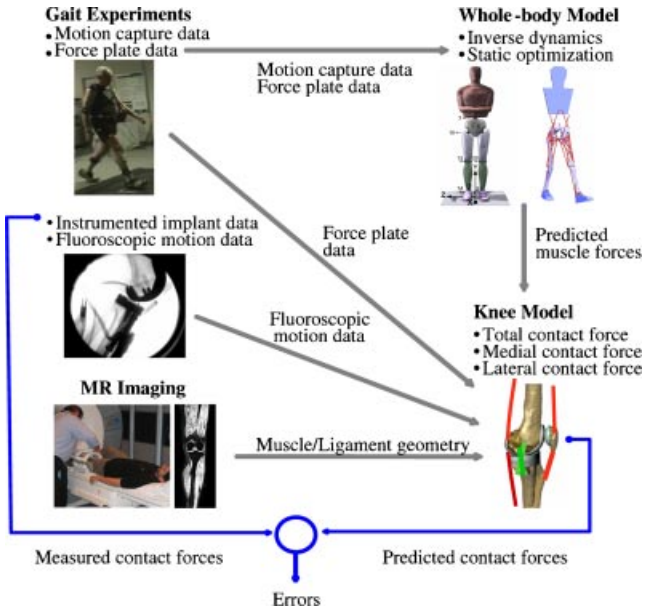

Figure 1. Diagram showing how modeling and experiments were integrated to determine knee-joint loading during gait. Motion capture and force plate data were input into a whole-body musculoskeletal model to calculate muscle forces in the lower limb. Force plate measurements of ground reaction forces, fluoroscopic measurements of tibiofemoral joint motion, and the calculated values of the muscle forces were then input into a 3D model of the implant to determine total, medial, and lateral tibial contact forces. The paths of the muscles and ligaments were obtained from MRI data recorded from a healthy adult male.

Measurements of the subject's joint motion and ground reaction forces were input into the whole-body model, and an inverse dynamics problem was solved to estimate the net moments exerted about the back, as well as each hip, knee, and ankle joint in the model. The net joint moments were decomposed into individual leg-muscle forces by solving an optimization problem that minimized the sum of the squares of the muscle activations at each instant of the gait cycle. The optimization solution was found subject to the physiological bounds on muscle force imposed by each muscle's force-length-velocity property.[13]

A separate 3D quasi-static knee model was developed to calculate the forces acting in the medial and lateral compartments of the implant. Six generalized coordinates were used to describe the configuration of the tibial and femoral components at each instant during the gait cycle. Flexion–extension, AP translation, and internal–external rotation were prescribed using the fluoroscopic data captured during the treadmill trials. Mediolateral translation of the tibia relative to the femur could not be measured accurately with single-plane fluoroscopy, and so this variable was set to zero in the model. The remaining two degrees of freedom (varus–valgus rotation and superior–inferior translation) were found by applying the contact conditions present at the tibiofemoral joint (see below).

The knee model was actuated by the same set of knee muscles incorporated in the whole-body model, except that vasti was separated into a medial, lateral, and intermediate portions. The geometry and mechanical behavior of the ligamentous and capsular structures were modeled using three separate bundles. The medial collateral ligament (MCL), lateral collateral ligament (LCL), and popliteofibular ligament (PFL) were each represented by one bundle. The ACL was not included in the analysis, as the patient had received a PCL retaining implant. The PCL was also excluded from the model, as this ligament bears force only at large flexion angles and therefore has little effect on knee-joint loading in stance.[17] The attachment sites of the muscles and ligaments were based on MRI data recorded from a young, healthy, adult male.

The model for patellofemoral mechanics constrained patellar motion to the sagittal plane. The position of the patella relative to the femur was described by three generalized coordinates: flexion–extension, AP translation, and superior–inferior translation. Assuming rigid contact between the patella and femur and an inextensible patellar tendon gave two algebraic equations, which were solved for the two patellar translations. Thus, patellofemoral mechanics was represented by just one equation, in which the orientation of the patella relative to the femur (flexion–extension) was the only unknown variable.

Hertzian contact theory was used to calculate the interpenetration between the tibial and femoral components, and the corresponding forces transmitted by the medial and lateral sides of the implant. The femoral condyles were modeled as spheres, each having a radius of 40 mm; the tibial plateau was approximated as a flat surface. The inputs to the knee model were the measured values of AP translation, flexion–extension, and internal–external rotation obtained from fluoroscopy; the

measured values of the three components of the ground reaction force and the location of the corresponding center of pressure; and the calculated values of the muscle forces obtained from optimization. The Hertzian contact model resulted in two algebraic equations, which were solved simultaneously for the values of the two unknown generalized coordinates of the tibiofemoral joint: varus–valgus rotation and superior–inferior translation. Once the configuration of the tibiofemoral joint was known, patellar position was found using the model of patellofemoral mechanics described above. Approximately 25 min of CPU time was needed on a 2.0 GHz desktop PC to determine the leg-muscle forces and the tibiofemoral contact forces for one gait cycle.

RESULTS

The sequence and timing of muscle activity predicted by the model was consistent with EMG measurements reported for normal walking (Fig. 2). Vasti and gastrocnemius generated the largest forces about the knee. The peak force developed by vasti was 448 N (0.73 BW), which occurred at contralateral toe-off. By comparison, the peak force in gastrocnemius was 743 N (1.1 BW), which occurred just before contralateral heel strike. The peak force in hamstrings was much smaller (441 N or 0.65 BW), and it occurred at heel strike. Some evidence of co-contraction between the quadriceps and hamstrings muscles was found. In particular, rectus femoris and medial hamstrings were activated simultaneously for a brief period immediately after heel strike (Fig. 2, RF and MHAMS).

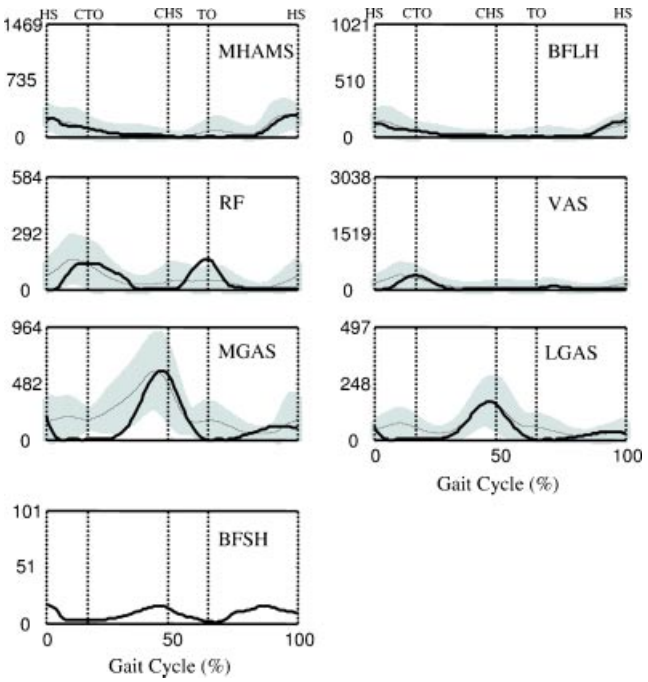

Figure 2. Knee muscle forces (thick lines) calculated for the TKA patient walking at his normal speed of 1.24 m/s. The gray shaded regions are EMG data[24] for healthy adults walking at an average speed of 1.36 m/s. The thin lines show the mean EMG data, while the gray regions indicate ± 1 SD. The muscle force plots are scaled to each muscle's maximum isometric strength. In the cases of RF, VAS, and BFSH, the muscle force plots are scaled to half the muscle's maximum isometric strength to provide a more effective scale for viewing the data. No EMG data were available for BFSH. Muscle symbols appearing in the plots are: MHAMS, medial hamstrings; BFLH, biceps femoris long head; RF, rectus femoris; VAS, vasti; MGAS, medial gastrocnemius; LGAS, lateral gastrocnemius; BFSH, biceps femoris short head. The vertical dashed lines signify key events: HS, heel strike; CTO, contralateral toe-off; CHS, contralateral heel-strike; TO, toe-off.

Strong qualitative and quantitative agreement were found between the calculated and measured tibial contact forces for each walking speed (Figs. 3 and 4). Over one full cycle of walking, the medial and lateral contact forces were predicted more accurately than the total tibial contact force. The average RMS error for the total contact force across all nine gait trials was 183 ± 45 N, which was 11% of the peak total force recorded by the instrumented knee. In contrast, the average RMS errors for the medial and lateral contact forces across all nine trials were 140 ± 40 N and 115 ± 32 N, respectively, which represented 14% and 16% of the peak contact forces measured in the medial and lateral compartments (Fig. 4, top panel). The RMS errors for stance were greater than those for swing. The average RMS error for the total contact force across all nine trials for stance was 204 ± 61 N, compared to 95 ± 17 N for swing. Similarly, the average RMS errors for the medial and lateral contact forces across all nine trials for stance were 149 ± 49 N and 121 ± 41 N, respectively, compared to 88 ± 35 N and 100 ± 35 N, respectively, for swing (Fig. 4, middle and bottom panels).

The agreement between model and experiment decreased as walking speed increased. RMS errors for the medial, lateral, and total contact forces all increased as the subject walked faster. The average RMS error for the total contact force increased from 145 N for a slow walk to 222 N for a fast walk. Similarly, RMS errors for the medial and lateral contact forces increased, respectively, from 93 N and 92 N for a slow walk to 174 N and 146 N for a fast walk (Fig. 4, top panel). The increase in RMS errors with walking speed occurred in both stance and swing.

DISCUSSION

Our aim was to evaluate the accuracy of knee muscle forces predicted for walking by comparing computed tibial contact forces against in vivo measurements obtained from an instrumented knee implant. While previous studies evaluated model predictions of muscle forces at the hip[5] and lumbar spine[8] using instrumented joint replacements, the present study is, to our knowledge, the first to evaluate muscle force estimates at the knee against direct measurements of tibiofemoral joint loading obtained in vivo from the same subject.

The model calculations of the medial, lateral, and total tibial contact forces were in close agreement with measurements obtained from one subject's instrumented knee implant for walking at slow, normal, and fast speeds (Figs. 3 and 4). Although these results show quantitatively that the model reproduced the time course of knee-joint loading for each of the three different walking speeds, this is a necessary, but not sufficient, condition for concluding that the corresponding knee

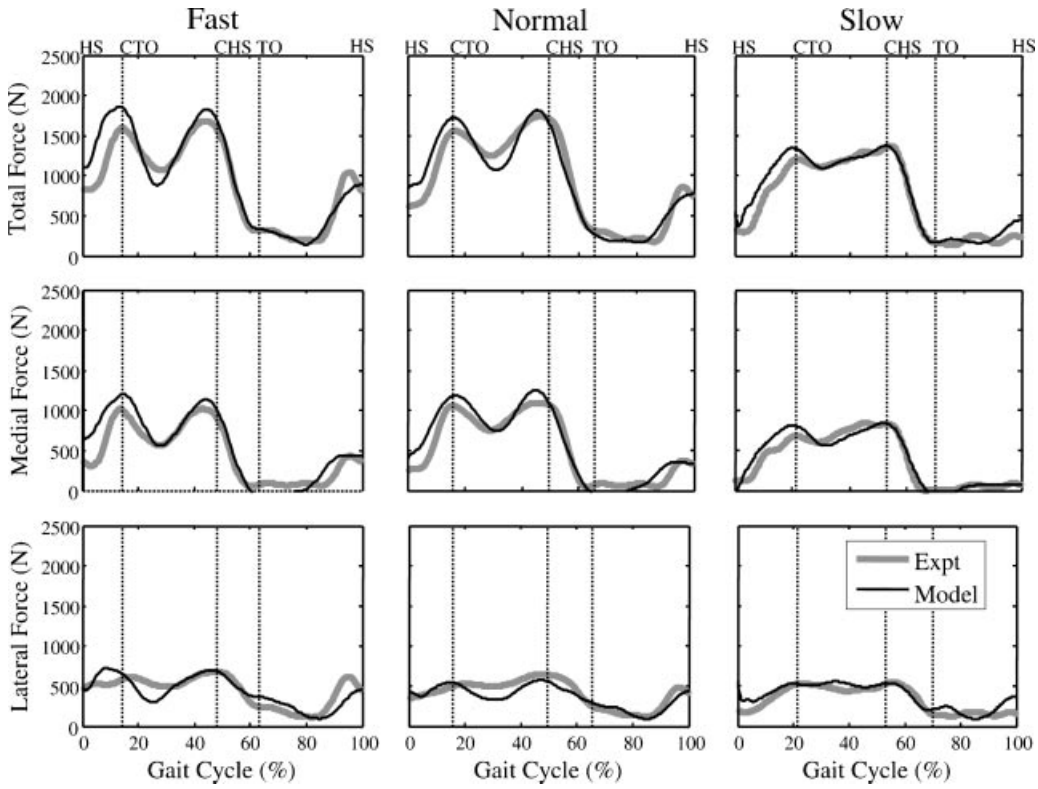

Figure 3. Tibial contact forces predicted by the model (black lines) for three walking speeds: slow (0.80 m/s), normal (1.24 m/s), and fast (1.52 m/s). The gray lines show measurements obtained from the TKA patient. Data are shown for one representative trial at each speed.

muscle forces were also determined accurately in the model. The reason is that 10 muscles crossing the knee in the model gave rise to the two contact forces calculated in the medial and lateral compartments of the tibiofemoral joint. This implies that many different combinations of knee muscle forces can yield the same pattern of tibiofemoral joint loading in the model, as is the case in life: the relationship between knee muscle forces and knee-joint loading is not unique. Nonetheless, we have confidence in our modeling results, as the muscle force patterns predicted for normal walking were also consistent with the sequence and timing of muscle activity obtained from EMG (Fig. 2).

Our study has a number of limitations that warrant consideration. In relation to the gait experiments, a potential inconsistency exists between the fluoroscopic data obtained from the treadmill experiments and the video motion and force plate data recorded in the over-ground walking trials. It was not possible to capture fluoroscopic data in the over-ground gait trials while video motion and force plate data were being recorded. Conversely, it was not possible to record ground force data during the treadmill experiments, as the treadmill was not instrumented with a force-measuring device.

The origin and insertion sites, and therefore moment arms, of the muscles in the knee model were based on MR data recorded from a healthy male subject who was similar in stature to the TKA patient. However, the force-producing properties of the muscles in the model (e.g., peak isometric muscle force and intrinsic maximum shortening velocity) were based on data reported for a generic model of the lower limb,[16] and the values of these parameters were not adjusted to account for the age and physical stature of the patient. Furthermore, the properties assumed for the ligaments in the model were based on data obtained from cadaver experiments.[17] It is difficult to know how the model predictions of leg-muscle forces and tibiofemoral joint loading may be affected by these approximations. In a recent study on the sensitivity of muscle force estimates to changes in muscle-tendon properties, Redl et al.[18] found that changes in the muscle-fiber length and tendon rest length of vasti were most critical to model estimates of leg-muscle forces in normal gait.

We also studied the sensitivity of knee-joint loading to changes in the values of the parameters assumed for the ligaments. Specifically, we altered the values of the reference lengths of the MCL, LCL, and PFL each by 10% of its nominal value, and recomputed the forces transmitted by the medial and lateral compartments of the knee for walking at the normal speed. A 10% increase in the reference length of the PFL decreased the peak values of the medial and lateral contact forces by 79 N (~0.11 BW) and 218 N (~0.31 BW), respectively. Similarly, a 10% increase in the reference length of the LCL decreased the peak values of the medial and lateral contact forces by 63 N (~0.09 BW) and 268 N (~0.38 BW), respectively. A 10% change in the reference length of the

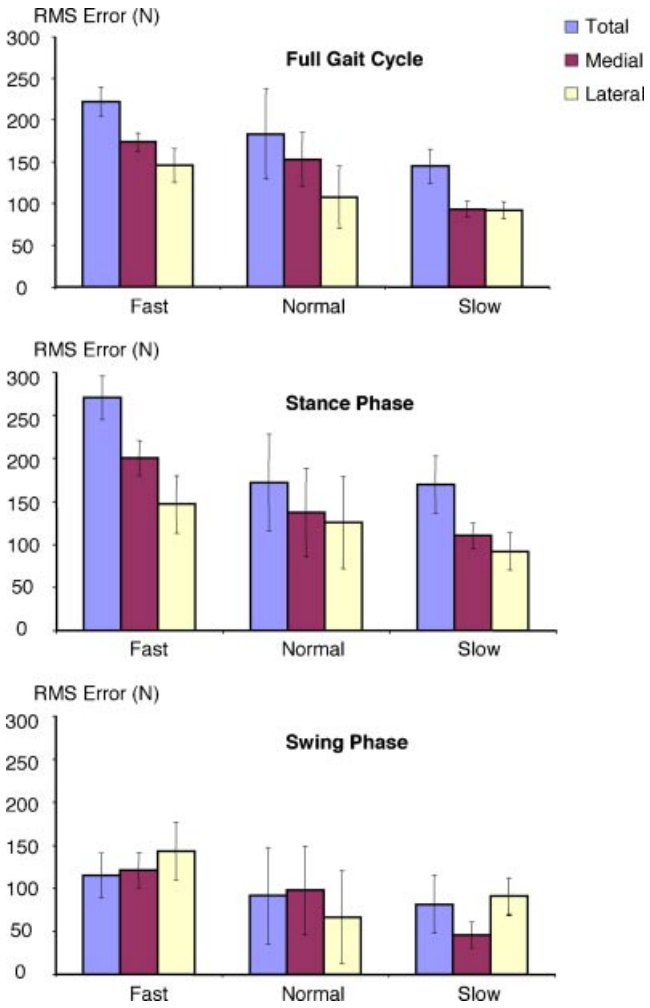

Figure 4. RMS errors for the model predictions of tibial contact force. Data are shown for the total, medial, and lateral contact forces calculated for the instrumented knee implant for all nine walking trials. Vertical lines on the bar graphs represent standard deviations of the errors.

MCL did not have a significant effect on knee-joint loading. These results suggest that changes in the reference lengths of the PFL and LCL are particularly important to model estimates of lateral compartment joint loading during gait. Future work should be directed at incorporating subject-specific musculoskeletal anatomy in a model of walking, and assessing the sensitivity of muscle and joint function to changes in musculoskeletal geometry and muscle, tendon, and ligament properties.

Our results showed that the lateral compartment remained loaded throughout the stance phase of walking, in contrast to some previous studies (e.g., Scuderi et al.[19]), which suggest that the lateral compartment may be unloaded during portions of stance. Several factors may determine whether condylar lift-off occurs in TKA gait, including implant design, surgical positioning of the implanted components, and differences in the walking biomechanics of individual subjects. With respect to differences in walking biomechanics, different subjects can exhibit different profiles of knee adduction moment during gait, and this difference can significantly influence the distribution of load across the knee.[20] While Scuderi et al.[19] reported the occurrence of condylar lift-off in 10 TKA patients, this phenomenon was not observed in the other 15 patients who participated in their study. The latter result is consistent with the way our TKA patient walked.

Our measurements of the total tibial contact force are consistent with data reported previously for walking at the normal speed. Taylor et al.[7] reported an average peak resultant tibiofemoral contact force of 3.1 BW, which is within the range measured in this study (1.9–3.5 BW). The calculated muscle forces are also in general agreement with the results of previous studies. Anderson and Pandy[14] estimated leg-muscle forces for normal walking by minimizing metabolic energy consumed per unit distance traveled. In their model, the knee muscles that developed the largest forces were vasti and gastrocnemius. The peak force in vasti was about 600 N at contralateral toe-off, while that in gastrocnemius was 700 N prior to contralateral heel-strike. The force calculated for hamstrings was about 400 N at heel-strike (see Figs. 5 and 6 in Anderson and Pandy[13]). In our study, the maximum resultant force estimated for vasti was 448 N at contralateral toe-off, while that for gastrocnemius was 539 N just before contralateral heel-strike. The peak resultant force calculated for hamstrings was 369 N at heel strike (Fig. 2).

The differences in peak muscle forces obtained in these two studies may be explained by the fact that the normal walking speed of the TKA patient was slightly lower than the average walking speed adopted by the participants in Anderson and Pandy's study (1.24 m/s vs 1.35 m/s, respectively). Further, the lower peak force calculated for vasti in the present study resulted from a lower peak knee-extension moment measured for the patient at contralateral toe-off, which is consistent with the observation that patients with knee osteoarthritis often adopt a quadriceps avoidance gait pattern that can persist subsequent to TKA.[21]

Finally, two factors may have contributed independently to the increased error observed in the tibial contact force predictions at the faster walking speeds (Fig. 4). First, the same cost function was used to estimate leg-muscle forces for all three speeds. Anderson and Pandy[13] found that a minimum-muscle-activation criterion yielded muscle forces similar in character to those obtained from a dynamic optimization solution that minimized metabolic energy consumption for walking at the normal speed. However, there is no reason to believe that a minimum-energy criterion would apply equally well to walking at higher speeds, where performance is more likely to be determined by muscle power production than muscle energy consumption. Second, skin motion artifact, and especially oscillation of the body markers immediately after heel strike, may have contributed significantly to inaccuracies in the estimated location of the knee joint center and, consequently, the calculated values of the lever arm of the ground reaction

force relative to the knee, the net moment exerted about the knee, and the forces produced in the knee muscles. The errors in the contact forces were largest during the initial period of stance (heel strike to contralateral toe-off). Tashman and Anderst[22] used markers mounted on bone pins to quantify the effects of skin-motion artifact subsequent to foot impact during one-legged hopping in humans. They found that skin-mounted markers oscillated by "bouncing" for a period of about 0.1 s subsequent to foot impact. This phenomenon might also attend in walking, particularly at higher speeds. We are currently using x-ray fluoroscopy to quantify the directional and temporal characteristics of skin-motion artifact, so that this information can be used to design improved skin-based marker sets for future gait analyses.[23]

ACKNOWLEDGMENTS

The authors gratefully acknowledge Dr. Darryl D'Lima and Dr. Cliff Colwell for providing the instrumented implant data and Dr. Scott Banks for providing the fluoroscopic motion data. This work was supported by an ARC Postdoctoral Fellowship (J. W. Fernandez), a VESKI Innovation Fellowship (M.G. Pandy), and an NSF CAREER Award (B. J. Fregly). Financial support was provided by the Australian Research Council under a Discovery Project Grant (DP0772838) and by National ICT Australia.

REFERENCES

1. Pandy MG. 2001. Computer modeling and simulation of human movement. Annu Rev Biomed Eng 3:245–273.
2. Shelburne KB, Torry MR, Pandy MG. 2006. Contributions of muscles, ligaments, and the ground-reaction force to tibiofemoral joint loading during normal gait. J Orthop Res 24: 1983–1990.
3. Brand RA, Pedersen DR, Davy DT, et al. 1994. Comparison of hip force calculations and measurements in the same patient. J Arthroplasty 9:45–51.
4. Heller MO, Bergmann G, Deuretzbacher G, et al. 2001. Musculo-skeletal loading conditions at the hip during walking and stair climbing. J Biomech 34:883–893.
5. Stansfield BW, Nicol AC, Paul JP, et al. 2003. Direct comparison of calculated hip joint contact forces with those measured using instrumented implants. An evaluation of a three-dimensional mathematical model of the lower limb. J Biomech 36:929–936.
6. Wilke HJ, Rohlmann A, Neller S, et al. 2003. ISSLS prize winner: A novel approach to determine trunk muscle forces during flexion and extension: a comparison of data from an in vitro experiment and in vivo measurements. Spine 28:2585–2593.
7. Taylor WR, Heller MO, Bergmann G, et al. 2004. Tibiofemoral loading during human gait and stair climbing. J Orthop Res 22:625–632.
8. Rohlmann A, Bauer L, Zander T, et al. 2006. Determination of trunk muscle forces for flexion and extension by using a validated finite element model of the lumbar spine and measured in vivo data. J Biomech 39:981–989.
9. Li G, Kawamura K, Barrance P, et al. 1998. Prediction of muscle recruitment and its effect on joint reaction forces during knee exercises. Ann Biomed Eng 26:725–733.
10. Zhao D, Banks SA, D'Lima DD, et al. 2007. In vivo medial and lateral tibial loads during dynamic and high flexion activities. J Orthop Res 25:593–602.
11. Zhao D, Banks SA, Mitchell KH, et al. 2007. Correlation between the knee adduction torque and medial contact force for a variety of gait patterns. J Orthop Res 25:789–797.
12. Banks SA, Hodge WA. 1996. Accurate measurement of three-dimensional knee replacement kinematics using single-plane fluoroscopy. IEEE Trans Biomed Eng 43:638–649.
13. Anderson FC, Pandy MG. 2001. Static and dynamic optimization solutions for gait are practically equivalent. J Biomech 34:153–161.
14. Anderson FC, Pandy MG. 2001. Dynamic optimization of human walking. J Biomech Eng 123:381–390.
15. Reinbolt JA, Schutte JF, Fregly BJ, et al. 2005. Determination of patient-specific multi-joint kinematic models through two-level optimization. J Biomech 38:621–626.
16. Anderson FC, Pandy MG. 1999. A dynamic optimization solution for vertical jumping in three dimensions. Comput Methods Biomech Biomed Eng 2:201–231.
17. Shelburne KB, Pandy MG, Anderson FC, et al. 2004. Pattern of anterior cruciate ligament force in normal walking. J Biomech 37:797–805.
18. Redl C, Gfoehler M, Pandy MG. 2007. Sensitivity of muscle force estimates to variations in muscle-tendon properties. Hum Mov Sci 26:306–319.
19. Scuderi GR, Komistek RD, Dennis DA, et al. 2003. The impact of femoral component rotational alignment on condylar lift-off. Clin Orthop Rel Res 410:148–154.
20. Shelburne KB, Torry M, Steadman JR, et al. 2008. Biomechanical effects of foot orthoses and valgus bracing on the knee adduction moment and medial joint load during gait. Clin Biomech 23:814–821.
21. Andriacchi TP, Natarajan RN, Hurwitz DE. 1997. Musculoskeletal dynamics, locomotion, and clinical applications. In: Mow VC, Hayes WC, editors. Basic orthopaedic biomechanics. 2nd ed. Philadelphia: Lippincott-Raven; p 37–68.
22. Tashman S, Anderst W. 2002. Skin motion artifacts at the knee during impact movements. In: Proceedings of the 7th Annual Meeting of the Gait and Clinical Movement Analysis Society, Chattanooga, TN.
23. Fernandez JW, Akbarshahi M, Kim HJ, et al. 2008. Integrating modelling, motion capture and x-ray fluoroscopy to investigate patellofemoral function during dynamic activity. Comput Methods Biomech Biomed Eng 11:41–53.
24. Winter DA. 1987. The biomechanics and motor control of human gait. Ontario, Canada: University of Waterloo Press; p 45.